Cancer Immunology, Immunotherapy (2021) 70:1227–1237
https://doi.org/10.1007/s00262-020-02747-w

ORIGINAL ARTICLE

Characterization of the tumor immune microenvironment in human papillomavirus-positive and -negative head and neck squamous cell carcinomas

Farah Succaria[1] · Pia Kvistborg[2] · Julie E. Stein[1] · Elizabeth L. Engle[3,4] · Tracee L. McMiller[4,5] · Lisa M. Rooper[6] · Elizabeth Thompson[4,6] · Alan E. Berger[5] · Michiel van den Brekel[2] · Charlotte L. Zuur[2] · John Haanen[2] · Suzanne L. Topalian[4,5] · Janis M. Taube[1,3,4]

Received: 18 February 2020 / Accepted: 12 October 2020 / Published online: 30 October 2020
© Springer-Verlag GmbH Germany, part of Springer Nature 2020

Abstract

Approximately 15% of advanced head and neck squamous cell carcinomas (HNSCC) respond to anti-PD-(L)1 monotherapies. Tumor PD-L1 expression and human papillomavirus (HPV) status have been proposed as biomarkers to identify patients likely to benefit from these treatments. We aimed to understand the potential immune effects of HPV in HNSCC and to characterize additional potentially targetable immune-regulatory pathways in primary, treatment-naïve tumors. CD3, CD4, CD8, CD20, CD68, FoxP3, PD-1, PD-L2, LAG-3, IDO-1, and GITR cell densities were determined in 27 HNSCC specimens. IHC for PD-L1 assessed percentage of positive tumor cells and immune cells separately or as a combined positive score (CPS), and whether PD-L1 was expressed in an adaptive or constitutive pattern (i.e., PD-L1+ tumor cells juxtaposed to TILs or in the absence of TILs, respectively). HPV testing with p16 IHC was confirmed by HPV genotyping. When compared to HPV(−) tumors ($n=14$), HPV+ tumors ($n=13$) contained significantly higher densities of CD3+, CD4+, CD8+, CD20+, and PD-1+ cells ($P<0.02$), and there was a trend towards increased density of FoxP3 + cells. PD-L1 expression patterns did not vary by tumor viral status, suggesting possible heterogeneous mechanisms driving constitutive vs adaptive PD-L1 expression patterns in HNSCC. IDO-1 expression was abundant (> 500 IDO-1+ cells/mm^2 in 17/27 specimens) and was found on tumor cells as well as immune cells in 12/27 (44%) cases (range 5–80% tumor cells+). Notably, the studied markers varied on a per-patient basis and were not always related to the degree of T cell infiltration. These findings may inform therapeutic co-targeting strategies and raise consideration for a personalized treatment approach.

Keywords Head and neck squamous cell carcinoma (HNSCC) · PD-1 · PD-L1 · HPV · IDO · GITR

Introduction

Head and neck squamous cell carcinoma (HNSCC) is a major cause of cancer morbidity and mortality worldwide [1]. It includes human papillomavirus-positive (HPV+) and -negative HPV(−) subtypes. In the United States, the incidence of HPV-associated HNSCC is on the rise [2]. Even with the use of multi-modality treatment regimens including surgery, chemotherapy, radiotherapy, and targeted therapy, approximately half of treated patients experience disease recurrence or progression [3].

Therapies blocking the PD-1:PD-L1 immune checkpoint pathway have improved progression-free and overall survival in a number of solid tumor types. There is great interest in optimizing this treatment approach in HNSCC. Clinical trials of anti-PD-1 in platinum-refractory recurrent/

Farah Succaria and Pia Kvistborg have contributed equally to this work.

Suzanne L. Topalian and Janis M. Taube have contributed equally to this work.

Electronic supplementary material The online version of this article (https://doi.org/10.1007/s00262-020-02747-w) contains supplementary material, which is available to authorized users.

✉ Janis M. Taube
jtaube1@jhmi.edu

Extended author information available on the last page of the article

metastatic HNSCC showed objective responses in ~ 15% of patients, and improved overall survival compared to salvage chemotherapy regimens, supporting FDA approvals for pembrolizumab and nivolumab in this treatment setting [3–5]. Patients with PD-L1+ compared to PD-L1 low/negative pretreatment tumor biopsies appeared to have higher response rates and prolonged survival [3, 5]. More recently, pembrolizumab was approved by the FDA for use in combination with chemotherapy (platinum and fluorouracil) as first-line therapy for all patients with advanced HNSCC, and as a single agent for patients whose tumors express PD-L1 (Combined Positive Score [CPS] ≥ 1) [6]. While HPV+ and HPV(−) HNSCCs contain similar mutational burdens [7], patients whose tumors express oncogenic HPV proteins have shown a trend towards improved overall survival following anti-PD-1 therapy [4], suggesting that foreign viral antigens might provoke strong antitumor immunity mediating tumor control. However, the majority of patients with HNSCC do not benefit from anti-PD-1 monotherapy, and there is a subset who experience rapid disease progression [8]. Mechanisms underlying primary or acquired resistance to anti-PD-1 are poorly understood. One possibility is that additional immunosuppressive pathways beyond PD-1:PD-L1 are operative within the tumor microenvironment (TME) [9, 10].

The purpose of this study was to characterize the HNSCC TME for expression of clinically targetable immune-regulatory markers beyond PD-(L)1, including the immunosuppressive molecules PD-L2, lymphocyte activation gene 3 (LAG-3), and indoleamine 2,3-dioxygenase 1 (IDO-1), and the costimulatory receptor glucocorticoid-induced TNFR-related protein (GITR), and to correlate their expression with densities of specific immune cell subsets and with tumor viral status. Importantly, while the expression of PD-L2, LAG-3, IDO-1, and GITR has previously been reported across HNSCCs [1, 11], here, we report distinct patterns of marker expression on a per-patient specimen basis.

Materials and methods

Case selection

Specimens were collected in compliance with the Institutional Review Boards of the Netherlands Cancer Institute (NKI) and Johns Hopkins University (JHU). Twenty-seven primary, treatment-naive HNSCC were identified in the NKI surgical pathology archives (acquired 1985–2014). The cohort clinicopathologic characteristics are shown in Table 1. A single representative formalin-fixed, paraffin-embedded (FFPE) block from each tumor specimen was chosen for further study and immunostains were performed on serial 5 µm-thick sections.

Human papillomavirus (HPV) status

Specimens were screened for p16 expression with immunohistochemistry (IHC) using the CINtec(c)p16^{INK4a} detection system (REF 9517; Roche Diagnostics, Tucson AZ, USA). Staining was performed according to the manufacturer's protocol, with the exception of a wash for 5 min in TBS containing 0.1% Tween 20 following the primary antibody incubation. "p16+" was defined as strong diffuse nuclear and cytosolic staining in > 70% of invasive tumor cells [12]. P16+ specimens then underwent HPV genotyping as previously described [13]. In brief, SPF-10 polymerase chain reaction (PCR) testing was performed at the Department of Pathology, Leiden University Medical Center. 10 um-thick sections were cut from each FFPE block using PCR-precautions. DNA was extracted, and an initial PCR generating a 150 base pair (bp) product was performed. Those generating a suitable product were advanced to an SPF-10 INNO-LiPA HPV PCR using the manufacturer's recommended protocol (Innogenetics NV, Ghent, Belgium). SPF-10-negative samples were labeled 'HPV-negative'. The SPF-10-positive samples were further tested to determine HPV subtype. They were first typed using an HPV16-specific PCR, and if negative for HPV16, were then advanced to typing using the INNO-LiPA HPV Genotyping Extra kit (Innogenetics NV, Ghent, Belgium).

Immunohistochemistry

Individual stains for CD3 (pan T cell), CD4 (T helper), CD8 (cytolytic T cell), CD20 (B cell), and CD68 (macrophage) were performed according to standard automated IHC methods. IHC for PD-L1 [14], PD-1 [15], LAG-3 [16], and GITR [17] was performed as previously described. Of note, the PD-L1 IHC was performed using the SP142 clone in a laboratory-developed test [14], and not the SP142 companion diagnostic test. The SP142 companion diagnostic assay detects less PD-L1 expression in both tumor cells and immune cells than other companion diagnostics, such as the 22C3, 28-8, and SP263 tests [18, 19]. However, when the SP142 antibody is optimized a laboratory-developed test with similar assay conditions to other key PD-L1 antibodies (22C3, 28-8, and SP263), it performs comparably with regard to tumor and immune cell detection of PD-L1. These findings were reported by two independent research groups in Sunshine et al. and Gaule et al. [14, 20], and indicate that it is the assay conditions in the SP142 companion diagnostic test that drive the differential performance and not the antibody itself.

The PD-L1 IHC assay used in the current study was the same laboratory-developed test described in Sunshine

Table 1 HNSCC patient and tumor characteristics

Specimen ID	Tumor anatomic location	Histologic subtype	Patient age at diagnosis (years)	Tumor stage[a]			Tumor HPV status[b]	Tumor cell PD-L1 status[c]	CPS for PD-L1[d]
				T	N	M			
1	Base of tongue	NK	38	3	0	0	+	–	10
2	Base of tongue	NK	45	3	0	0	+	–	20
3	Tonsil	NK	70	3	0	0	+	–	10
4	Tonsil	NK	61	1	2B	0	+	–	20
5	Tonsil	C	73	4A	2B	0	–	–	20
6	Tonsil	C	64	2	0	0	–	–	0
7	Base of tongue	NK	60	4A	2C	0	–	–	10
8	Base of tongue	C	63	2	0	0	–	–	20
9	Base of tongue	C	28	4	0	0	+	+	10
10	Base of tongue	NK	53	2	1	0	+	+	20
11	Tonsil	NK	61	3	3	0	+	+	100
12	Base of tongue	NK	51	2	2A	0	+	+	100
13	Tonsil	NK	71	1	2A	0	+	+	20
14	Tonsil	NK	61	1	1	0	+	+	60
15	Tonsil	C	49	4A	2B	0	+	+	20
16	Tonsil	NK	56	1	1	0	+	+	50
17	Tonsil	NK	51	2	2B	0	+	+	90
18	Oropharynx	C	34	4A	0	0	–	+	40
19	Base of tongue	C	39	4B	1	0	–	+	20
20	Base of tongue	C	34	4A	2	0	–	+	100
21	Base of tongue	C	51	4	0	0	–	+	50
22	Tonsil	C	64	3	3	0	–	+	5
23	Soft palate	C	50	4	2C	0	–	+	10
24	Tonsil	C	56	4	3	0	–	+	5
25	Tonsil	NK	57	3	2C	0	–	+	10
26	Tonsil	C	55	4B	2B	0	–	+	40
27	Tonsil	C	74	3	2B	0	–	+	70

NK non-keratinizing, *C* conventional

[a]American Joint Committee on Cancer (AJCC) staging

[b]HPV status determined by p16 IHC and confirmed by HPV genotyping, as described in Methods. All had the HPV16 genotype except for tumor #14, which was HPV58

[c]Tumors are defined as PD-L1 + if ≥ 5% of tumor cells express membranous (cell surface) PD-L1 by IHC

[d]CPS is defined as the percentage of PD-L1 TCs and ICs relative to the total number of tumor cells

et al. [14]. Specifically, antigen retrieval was performed for 10 min at 120 °C (Decloaking chamber, Biocare Medical) using a citrate buffer, pH 6.0 (Dako S1699). Endogenous peroxidases, protein, and biotin were blocked (Fisher Scientific H325–500, Serotec Block ACE, and Vector Avidin/Biotin Blocking Kit, respectively), and the primary antibody (SP142, Spring Bioscience) was applied at a concentration of 0.096 µg/mL and allowed to incubate at 4 °C for 22 h. The slides were then washed, and a biotinylated anti-rabbit IgG (BD Biosciences) secondary antibody was applied at 1.0 µg/mL and allowed to incubate for 30 min at room temperature. Signal was developed using an ABC Kit (Vector Elite PK-6100), followed by amplification with the TSA Plus Biotin Kit (Perkin Elmer). Samples were visualized with Streptavidin-HRP, followed by DAB chromogen and a hematoxylin counterstain.

IHC for FOXP3 (T regulatory cells; Tregs), PD-L2, and IDO-1 was performed using monoclonal antibodies, Table 2.

Table 2 Primary monoclonal antibodies used for FOXP3, PD-L1, PD-L2, and IDO-1 IHC

	Clone	Source	Staining concentration
FoxP3	236A/E7	Abcam	10 µg/mL
PD-L1	SP142	Spring Bioscience	0.096 ug/mL
PD-L2	F04	Bristol–Myers Squibb	1 µg/mL
IDO-1	SP260	Spring Bioscience	1.19 µg/mL

Antigen retrieval was performed by ER2 (Leica Biosystems), and signal was developed by Bond Polymer Refine Detection (Leica Biosystems). Appropriate positive and negative controls were performed for all IHC assays.

Scoring of immune cell subsets and immune coregulatory molecule expression

Membranous (cell surface) PD-L1 expression on tumor or infiltrating immune cells was scored visually by a board-certified pathologist as previously described [16] at approximately 0, 5%, 10%, and increasing 10% intervals. PD-L1 expression on ≥ 5% cells among tumor cells (TCs) or immune cells (ICs) was considered positive for that cell type. Intensity of immune cell infiltrates was graded as none (0), mild (1, rare lymphocytes), moderate (2, infiltration of tumor periphery or extending away from perivascular regions), or severe (3, diffuse infiltration or dense infiltrate surrounding the complete tumor perimeter). Geographic association of tumor cell PD-L1/-L2 expression and immune infiltrates was described by the following patterns: constitutive expression (PD-L expression without immune cell infiltrates), adaptive (PD-L only in areas of immune cell infiltration), or mixed (broad areas of constitutive PD-L expression, with enhancement in areas of immune cell infiltration). A combined proportion score (CPS) for PD-L1 expression was also assigned for each case. CPS is defined as the percentage of PD-L1(+) TCs and ICs relative to the total number of TCs.

Immunostained slides were scanned at 20× objective equivalent (0.49 microns per pixel) using a Nanozoomer XR (Hamamatsu Photonics, Hamamatsu City, Japan). The TME (inclusive of tumor cells and 200 µm of peritumoral stroma) was annotated by a pathologist. Necrotic, folded, or fragmented areas were excluded. Digital image analysis with HALO Immune Cell Module software (Indica Labs) was used to quantify marker-positive cell densities, i.e., number of positive cells/mm^2, using best-fit parameters for CD3, CD4, CD8, CD20, CD68, FOXP3, PD-1, PD-L2, LAG-3, IDO-1, and GITR. For markers that were expressed by both tumor and immune cells, marker-positive immune cell densities were calculated by subtracting the estimated percent of positive tumor cells from the total marker-positive cell density. The patterns and prevalence of immune cell infiltrates and coregulatory molecule expression were then studied as continuous variables on a per-patient specimen basis and tested for an association with tumor viral status. Patterns of PD-L1 expression were also tested for an association with tumor viral status and infiltrating CD3+ T cell densities.

Results

Patient characteristics and tumor specimens

The median age of patients at diagnosis was 56 years; 85% were current or former smokers, and 78% consumed alcohol. Among 27 tumor specimens, 16 (59%) expressed p16 protein by IHC, and 13/27 (48%) were subsequently deemed to be HPV+ by viral genotyping (twelve HPV16, one HPV58). Therefore, this study includes 13 HPV+ and 14 HPV(−) tumors. 85% (11/13) of the HPV+ tumors were non-keratinizing, and 86% (12/14) of the HPV(−) tumors had a conventional histology ($P = 0.0004$, Fisher's exact test), supporting the alignment of histology with HPV status [21]. There was no significant association between HNSCC histologic subtype and tumor cell PD-L1 expression ($P = 0.42$, Fisher's exact test) (Table 1).

PD-L1 and PD-L2 expression by tumor cells

PD-L1 expression was abundant in the HNSCC TME, with an average CPS of 35%. Nineteen of 27 specimens (70%) had ≥ 5% PD-L1+ tumor cells, including 9 HPV+ and 10 HPV(−) cases (Table 1). Among 23 tumors expressing PD-L1 on ≥ 5% tumor cells, 22% (5/23) exhibited a constitutive expression pattern (PD-L1+ tumor cells in the absence of TILs), 52% (12/23) displayed an adaptive expression pattern (PD-L1+ tumor cells juxtaposed to TILs), and 26% (6/23) had a mixed pattern (Fig. 1a–c, respectively). There was no significant correlation between tumor cell PD-L1 expression or PD-L1 CPS and CD3+, CD4+, or CD8+ T cell densities, most likely reflecting a component of constitutive PD-L1 expression in ~ 50% of the HNSCC cases in this cohort (Fig. 1d and Supplementary Fig. 1 for CD3+, CD4+, and CD8+ data not shown). The proportion of specimens showing each of the tumor cell PD-L1 expression patterns was not associated with tumor viral status ($P = 0.75$, Fisher's exact test) (Fig. 1e). PD-L2 expression, when observed, had an adaptive pattern (15/15 specimens), with 13% (2/15) specimens also demonstrating a component of constitutive tumor cell expression.

Immune cell infiltration and expression of immune coregulatory molecules in the HNSCC TME

All HNSCC specimens contained infiltrating immune cells, scored as 1+ to 3+ according to intensity and location [22]. Notably, immune cells expressed PD-L1 in 26/27 (96%) specimens (range 5–80% of immune cells PD-L1+). The proportion of PD-L1+ immune cells often exceeded PD-L1+ tumor cells, and, in some cases, occurred even in

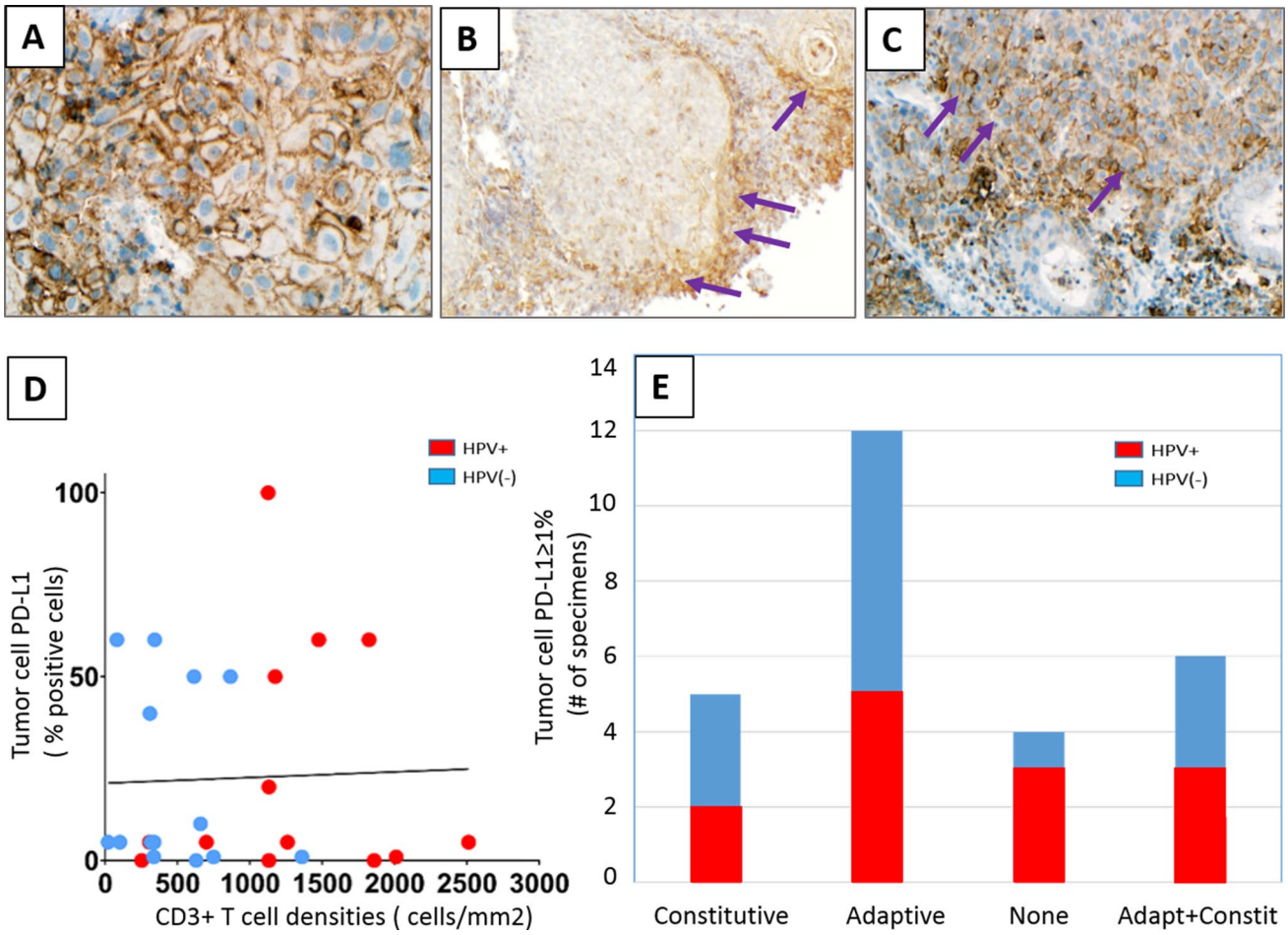

Fig. 1 Patterns of PD-L1 expression in HNSCC. Representative examples of **a** constitutive adaptive, **b** adaptive, and **c** combined constitutive and adaptive (mixed) patterns of tumor cell PD-L1 expression are shown. PD-L1 staining is marked by brown chromogen. Purple arrows mark areas of adaptive tumor cell PD-L1 expression at the interface with infiltrating lymphocytes. **d** There was no significant correlation between tumor cell PD-L1 expression and infiltrating CD3+ T cell densities ($r = -0.0358$, $P = 0.86$) or PD-L1 CPS and CD3+ cell densities ($r = 0.21$, $P = 0.29$, see Supplementary Fig. 1 for CPS figure), consistent with the finding of constitutive tumor cell PD-L1 expression in many cases. **e** Distinct patterns of tumor cell PD-L1 expression in HNSCC specimens did not correlate with tumor viral status. 400×, 100×, and 200×, original magnifications for panels **a**, **b**, and **c**, respectively

the complete absence of tumor cell PD-L1 expression. Neither the proportion of tumor cells nor infiltrating immune cells expressing PD-L1 differed significantly between positive and negative tumor viral status ($P = 0.89$ and 0.27, respectively, Wilcoxon rank-sum test).

The HNSCC TME contained, on a per-specimen basis, varying densities of immune cells expressing CD3, CD4, CD8, CD20, CD68, FOXP3, PD-1, PD-L2, LAG-3, IDO-1, and GITR. Individual cases showed distinct intensities and patterns of immune coregulatory molecule expression. For example, as shown in Fig. 2, specimens #4 and #8 both contained T cell inflammation (CD3+ cells) with prominent PD-1 expression. However, specimen #8 contained LAG-3+ and GITR+ immune cell populations proportionate to PD-1 expression, while specimen #4 had notably fewer LAG-3+ cells. Low-level GITR expression by tumor cells was also seen in specimen #4, representative of 4/27 (15%) specimens in this study.

Of note, although IDO-1 is often described as being expressed by myeloid cells, it was expressed by tumor cells as well as immune cells in 12/27 (44%) HNSCC cases, with 5–80% of all IDO-1+ cells being tumor cells. IDO-1 staining patterns differed across specimens (Fig. 3). For example, specimen #8 showed constitutive tumor cell IDO-1 staining, whereas specimen #4 showed prominent IDO-1 display at the tumor–host interface in tumor cells, CD68+ macrophages, and lymphocytes. Distinct histopathologic patterns of IDO-1 expression were observed among 25/27 specimens that had ≥ 5% positive cells: (1) focal tumor–host interface expression (mostly immune cells and rare tumor cells) in 18/27 (67%) cases; (2) complete tumor–host interface (immune cells and tumor cells) in 4/27 (15%); and (3)

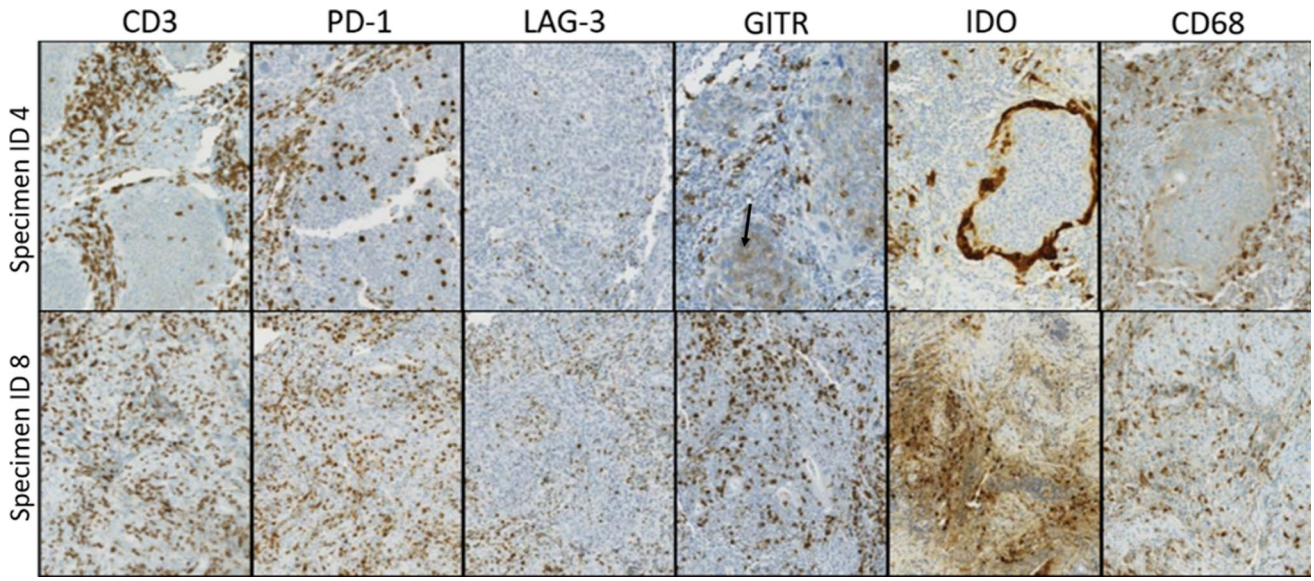

Fig. 2 Patterns and prevalence of immune cell infiltrates and coregulatory molecule expression vary by HNSCC specimen. Individual tumor specimens showed varied expression of different markers. For example, both specimens #4 and #8 (top and bottom rows, respectively) are CD3+ T cell inflamed tumors with prominent PD-1 expression. However, specimen #8 also shows LAG-3+ and GITR+ immune cell populations proportionate to PD-1 expression, while specimen #4 has notably less LAG-3 expression. Low-level GITR expression by tumor cells is also present in specimen #4 (black arrow). Additionally, IDO-1 staining patterns differed across specimens. For example, specimen #8 shows constitutive tumor cell IDO-1 expression, whereas specimen #4 shows prominent IDO-1 display at the tumor–host interface in an adaptive pattern

constitutive (broad tumor cell expression, independent of the degree of infiltrating immune cells) in 3/27(11%). Since IDO-1 expression can be induced by interferon-gamma, the interface patterns suggest adaptive expression in response to cytokine secretion by local, activated T cells. Neither tumor cell nor immune cell IDO-1 expression differed by HPV status.

Computer-assisted quantification of densities of immune cell subsets and coregulatory molecule expression

Image analysis was used to quantify densities of immune cell subset and coregulatory marker expression for each tumor specimen. The specimens were then ranked by relative CD3+ T cell densities, as represented by a color gradient (Fig. 4). CD4+, CD8+, CD20+, FOXP3+, PD-1+, and LAG-3+ cell densities all increased with increasing CD3+ T cell densities. In contrast, densities of immune cells expressing PD-L2, IDO-1, or GITR did not correlate with T-cell density, perhaps reflecting constitutive tumor cell expression as described above. IDO-1 and GITR expression were relatively abundant across the specimens (> 500 marker-positive immune cells/mm^2 in 16/27 and 17/27 specimens, respectively). Notably, individual patients showed strikingly different levels and patterns of PD-L2, IDO-1, and GITR expression.

Association of tumor HPV status with infiltrating immune cell subsets and coregulatory marker expression

When compared to HPV(−) tumors, HPV + tumors contained significantly higher densities of CD3+, CD4+, CD8+, CD20+, and PD-1+ cells; there was also a trend towards an increased density of FOXP3+ cells in HPV+ tumors (Fig. 5). Furthermore, when examining only PD-L1+ tumors, these markers remained significantly higher in HPV+ vs. (−) tumors (data not shown). In contrast, when comparing specimens in which tumor cells were PD-L1+ vs. PD-L1(−), there were no significant differences in immune cell densities (data not shown), consistent with our finding of constitutive PD-L1 expression in many of these tumors**.**

Discussion

Despite the availability of anti-PD-1 drugs, platinum-refractory recurrent/metastatic HNSCC remains a treatment challenge, and first-line anti-PD-1 monotherapy or chemotherapy combination benefits only a proportion of patients. As such, there is great interest in developing new immunotherapy strategies for patients with HNSCC, and numerous clinical trials are currently underway. Previous studies of large datasets, including TCGA analysis [1], have shown that multiple

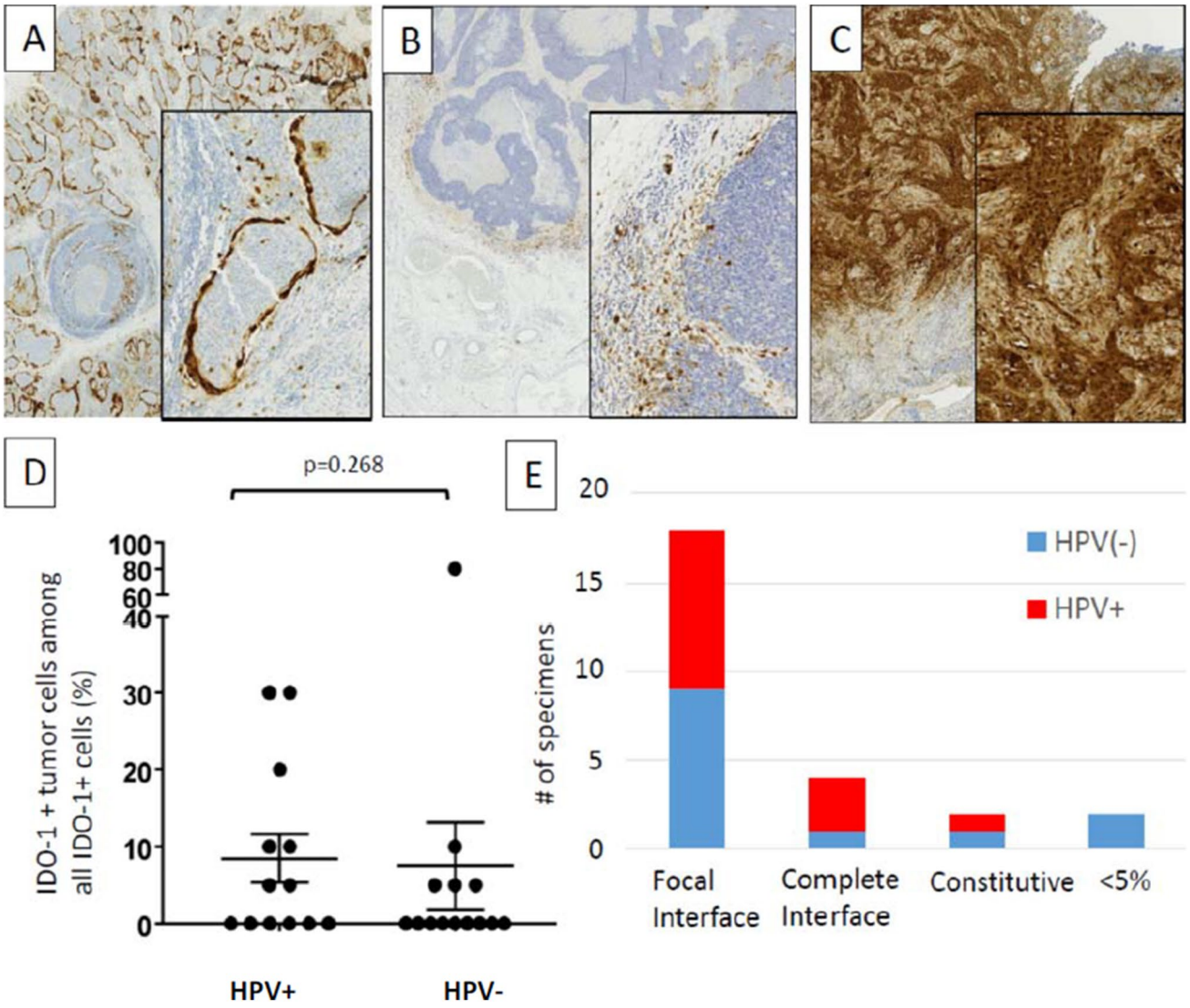

Fig. 3 Patterns of IDO expression in the TME of HNSCC. Distinct patterns of IDO cell expression were observed including **a** complete interface pattern (tumor islands ringed by IDO + tumor cells and macrophages), **b** focal interface pattern (predominantly immune cell expression with rare tumor cell expression), and **c** constitutive tumor cell expression. There was no statistical significance of **d** tumor cell expression or **e** expression pattern between HPV + and HPV(−) HNSCC specimens

checkpoints are expressed in HNSCC; however, an understanding of the interrelationship of these markers in situ and on an individual patient basis is still lacking. In the current study, we demonstrate that the immune microenvironment of HNSCC is heterogeneous, being characterized by various immune cell populations and coregulatory molecules which are not always dependent on viral status or the degree of inflammation in the TME.

Viral oncoproteins have been proposed as a marker of tumors susceptible to PD-1 blockade. Both HPV + and HPV(−) HNSCC tumors have an immune-active TME. Our findings that HPV + tumors had significantly increased densities of CD3+, CD4+, CD8+, CD20+, and PD-1 + cells compared to HPV(-) cases are in keeping with previous reports [1, 23]. Markers of immune activation (perforin and granzyme A and B) and CD56+ natural killer cells have also been observed to be elevated in HPV + compared to HPV(−) HNSCC [1]. Taken together, these findings suggest a stronger intratumoral immune reaction in the presence of the HPV oncogenic virus, which may explain the markedly better prognosis associated with HPV + HNSCC compared with HPV(−) tumors [24], and improved overall survival following anti-PD-1 therapy [4, 6].

The expression of PD-L1 in the TME has been widely studied as a prognostic biomarker as well as a predictor of therapeutic response to anti-PD-1. Patients with chemotherapy-refractory PD-L1 + HNSCC who received anti-PD-1 therapies appeared to have prolonged overall survival,

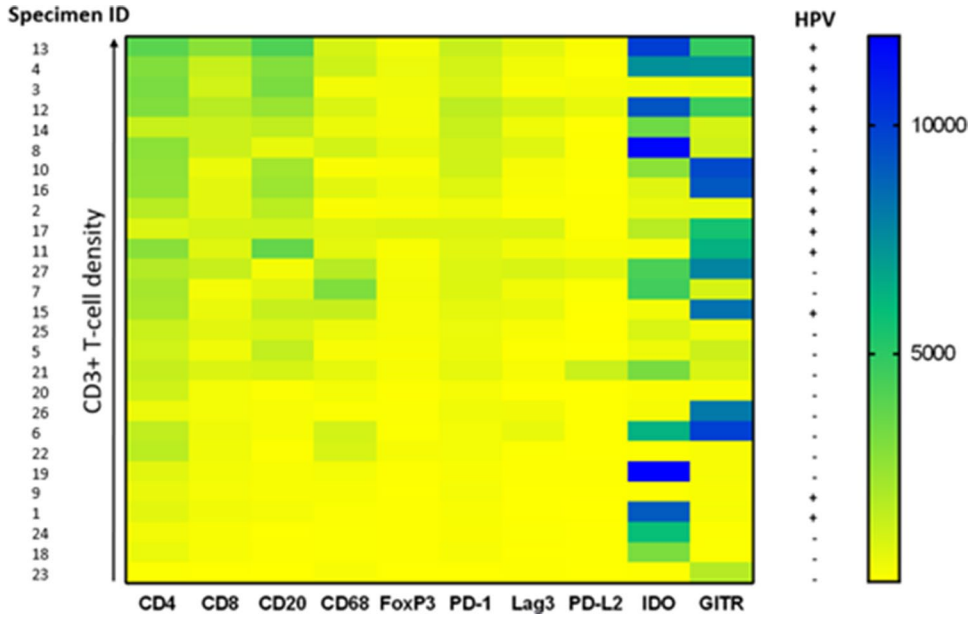

Fig. 4 Correlation of degree of intratumoral CD3+ T cell infiltration with immune cell subset densities and coregulatory marker expression. Colors indicate density of marker-positive immune cells. All 27 HNSCC specimens are ranked by CD3+ T cell densities, and specimen IDs are provided to the left of the figure. HPV status is provided to the right

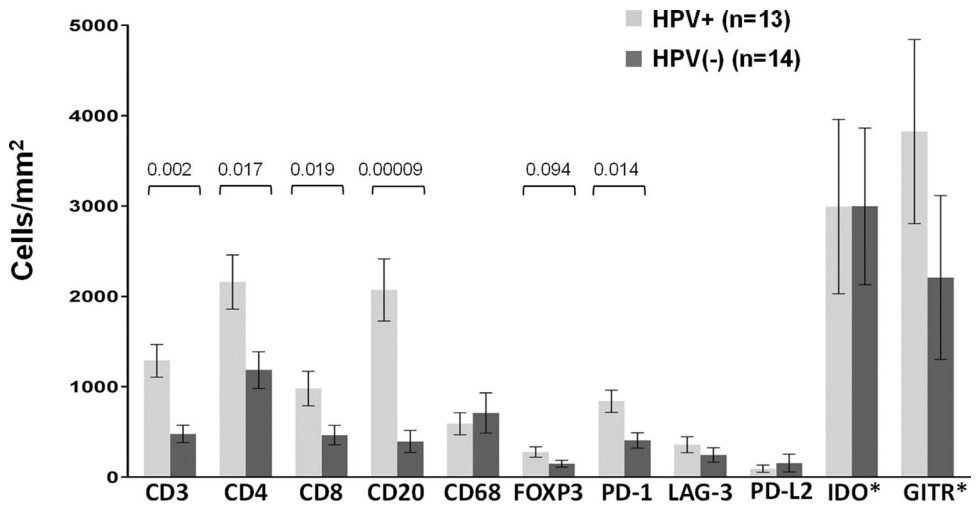

Fig. 5 Immune cell subsets and coregulatory molecule expression on immune cells in HPV+ vs. HPV(−) HNSCC. Protein marker expression was detected with immunohistochemistry and analyzed digitally, as detailed in "Materials and methods". When compared to HPV(−) tumors, HPV+ tumors contained significantly higher densities of CD3+, CD4+, CD8+, CD20+, and PD-1+ cells; there was also a trend towards an increased density of FOXP3+ cells in HPV+ tumors. Expression of IDO-1 and GITR by immune cells was robust, but did not differ by tumor viral status. P-values, 2-sided Wilcoxon rank-sum test with exact distribution. Error bars display mean ± SEM

compared to those with PD-L1 low/negative tumors [3, 5]. Furthermore, in the front-line setting, pretreatment tumor PD-L1 expression is FDA-approved as a biomarker to select patients with advanced HNSCC for anti-PD-1 monotherapy [6]. In the current report, the TME in both HPV+ and HPV(−) HNSCC contained abundant PD-L1 expression on tumor and/or immune cells. Of note, different patterns of tumor cell PD-L1 expression were observed (adaptive, constitutive, or mixed), which did not correlate with viral status. These different patterns provide insight as to why binary PD-L1 "status" (positive vs. negative with respect to a given threshold) may not perform well as a solitary biomarker in HNSCC [25]. It is also possible that a marker such as PD-1/PD-L1 distance, which can help separate adaptive from constitutive expression, may be more specific for identifying patients likely to respond to anti-PD-(L)1 therapy [26].

PD-L2, the second ligand for the PD-1 receptor, is also recognized as playing a role in local immunosuppression within the TME by downregulating T cell activation following engagement with PD-1 [27]. PD-L2 expression has been described on immune as well as tumor cells. PD-L2 protein expression is not as well characterized as for PD-L1,

although some studies on its prognostic and predictive implications have been performed. One study showed that PD-L2 is a poor prognostic marker for p16(−) HNSCC patients [28]. Another showed that PD-L2 expression detected by IHC had additive value over PD-L1 status alone in predicting response to anti-PD-1 in patients with HNSCC [11]. In the current study, some degree of PD-L2 expression was detected in nearly every tumor specimen, but this was quite variable (range 3–1270 positive cells/mm^2). PD-L2 expression did not correlate with viral status, nor with CD3+ T cell densities. The development of PD-L2 as a biomarker may benefit from an analysis of whether the distance between PD-1+ and PD-L2+ cells is more predictive of treatment outcomes than PD-L2 status alone.

Regulatory T cells (Tregs) are thought to play an immunosuppressive role in the TME during tumor development and may potentially antagonize anti-cancer strategies. In a comparison of 10 different tumor types using the TCGA dataset, HNSCC expressed the highest level of Treg markers, suggesting that therapies targeting Tregs may be of specific interest in this tumor type [1]. Here, we found that Tregs were present in both HPV+ and HPV(−) HNSCC tumors, with a trend towards increased density in HPV+ cases. Two of the immunoactive molecules studied here, IDO-1 and GITR, are thought to modulate the Treg population, i.e., IDO facilitates the proliferation and activation of Tregs by decreasing bioavailable tryptophan within the TME [29], while GITR inhibits Treg-mediated immunosuppression by reducing IL-10 secretion and inducing CD8+ T cell expansion [30]. In our study, IDO-1 expression was relatively abundant and was expressed by tumor cells as well as immune cells in 44% of cases. There was also a broad range of GITR expression, which, in some cases, was expressed at a higher density than IDO-1. The inter-patient heterogeneity of immune coregulatory molecule expression as well as the extent of IDO-1 and GITR expression in certain cases was particularly notable, suggesting that targeted inhibition of IDO-1 or stimulation of GITR in select patients may help reverse Treg-mediated immunosuppression within the TME. In the future, additional insights may be potentially be gained using emerging multiplexing technologies to characterize immunoactive protein patterns of co-expression on a single-cell basis, in addition to the patterns across the entire TME reported here [31].

In conclusion, this study suggests a stronger immune response against HPV+ compared to HPV(−) HNSCC tumors, but no significant difference according to tumor cell PD-L1 status or CPS. It also suggests that different expression profiles of various immune-regulatory molecules occur in individual tumors. There are currently many ongoing clinical trials that pair anti-PD-1 with one or more additional coregulatory agonists/antagonists. Although based on a modest-sized cohort, our findings suggest that a personalized combination immunotherapy approach to HNSCC based on characterizing each patient's unique TME may be warranted. Trials investigating the safety and feasibility of utilizing real-time tumor profiling to select specific immunotherapeutic agents for patients are currently underway [32]. Our findings suggest that an adaptive trial design for testing the next generation of immunotherapeutic regimens may be of particular value in patients with advanced HNSCC.

Acknowledgements The authors would like to acknowledge Drs. Robin Edwards and Darren Locke (Bristol-Myers Squibb) for helpful discussions and provision of the PD-L2 antibody.

Funding This work was supported by the Bristol-Myers Squibb (PK, JH, SLT, JMT); National Cancer Institute R01 CA142779 (SLT, JMT); NIH T32 CA193145 (JES); and the Johns Hopkins Bloomberg-Kimmel Institute for Cancer Immunotherapy.

Data availability The datasets generated during the current study are available from the corresponding author on reasonable request.

Compliance with ethical standards

Conflict of interest J. M. Taube reports consulting/advisory board for BMS, Merck, AstraZeneca, and Compugen; research funding through Bristol Myers Squibb; and reagents and machine loan from Akoya Biosciences. S. L. Topalian reports stock and other ownership interests in Aduro Biotech, DNAtrix, Dracen Pharmaceuticals, Dragonfly Therapeutics, Ervaxx, Five Prime Therapeutics, Potenza Therapeutics, RAPT, Tizona Therapeutics, Trieza Therapeutics, and WindMIL; a consulting or advisory role in Amgen, DNAtrix, Dragonfly Therapeutics, Dynavax, Ervaxx, Five Prime Therapeutics, Immunocore, Immunomic Therapeutics, Janssen Pharmaceuticals, MedImmune/AstraZeneca, Merck, RAPT, and WindMIL; research grants from Bristol Myers Squibb and Compugen; patents, royalties, and/or other intellectual property through her institution with Aduro Biotech, Arbor Pharmaceuticals, Bristol Myers Squibb, Immunomic Therapeutics, NexImmune, and WindMIL; and travel, accommodations, and expenses from Bristol-Myers Squibb and Five Prime Therapeutics. P. Kvistborg is a consultant for Neon Therapeutics and Personalis and a recipient of grant/research support from Bristol-Myers Squibb and Merck. J. Haanen: NKI received financial compensation for advisory role of J. Haanen with AZ, Amgen, Bayer, BMS, Celsius Therapeutics, MSD, Merck Serono, Pfizer, Roche/Genentech, Neon Therapeutics, Immunocore, Seattle Genetics, Novartis, GSK. Also, NKI received research grants through J. Haanen from BMS, MSD, Novartis, and Neon Therapeutics. J. Stein reports consulting (uncompensated) for AstraZeneca. No potential conflicts of interest were disclosed by the other authors.

Ethical approval The local Ethics Committees of the Netherlands Cancer Institute (NKI) and Johns Hopkins University (JHU) approved this study. The study is retrospective in nature and all procedures performed were part of routine care.

References

1. Mandal R, Senbabaoglu Y, Desrichard A, Havel JJ, Dalin MG, Riaz N et al (2016) The head and neck cancer immune landscape and its immunotherapeutic implications. JCI Insight 1:e89829

2. Chaturvedi AK, Engels EA, Pfeiffer RM, Hernandez BY, Xiao W, Kim E et al (2011) Human papillomavirus and rising oropharyngeal cancer incidence in the United States. J Clin Oncol 29:4294–4301
3. Ferris RL, Blumenschein G Jr, Fayette J, Guigay J, Colevas AD, Licitra L et al (2016) Nivolumab for recurrent squamous-cell carcinoma of the head and neck. N Engl J Med 375:1856–1867
4. Chow LQ, Haddad R, Gupta S, Mahipal A, Mehra R, Tahara M et al (2016) Antitumor activity of pembrolizumab in biomarker-unselected patients with recurrent and/or metastatic head and neck squamous cell carcinoma: results from the phase Ib KEYNOTE-012 expansion cohort. J Clin Oncol 34:3838–3845
5. Cohen EEW, Soulieres D, Le Tourneau C, Dinis J, Licitra L, Ahn MJ et al (2019) Pembrolizumab versus methotrexate, docetaxel, or cetuximab for recurrent or metastatic head-and-neck squamous cell carcinoma (KEYNOTE-040): a randomised, open-label, phase 3 study. Lancet 393:156–167
6. Burtness B, Harrington KJ, Greil R, Soulières D, Tahara M, de Castro, Jr G et al (2019) Pembrolizumab alone or with chemotherapy versus cetuximab with chemotherapy for recurrent or metastatic squamous cell carcinoma of the head and neck (KEYNOTE-048): a randomised, open-label, phase 3 study. Lancet 394:1915–1928
7. Seiwert TY, Zuo Z, Keck MK, Khattri A, Pedamallu CS, Stricker T et al (2015) Integrative and comparative genomic analysis of HPV-positive and HPV-negative head and neck squamous cell carcinomas. Clin Cancer Res 21:632–641
8. Saada-Bouzid E, Defaucheux C, Karabajakian A, Coloma VP, Servois V, Paoletti X et al (2017) Hyperprogression during anti-PD-1/PD-L1 therapy in patients with recurrent and/or metastatic head and neck squamous cell carcinoma. Ann Oncol 28:1605–1611
9. Zou W, Wolchok JD, Chen L (2016) PD-L1 (B7–H1) and PD-1 pathway blockade for cancer therapy: mechanisms, response biomarkers, and combinations. Sci Transl Med. 8:328rv324
10. Koyama S, Akbay EA, Li YY, Herter-Sprie GS, Buczkowski KA, Richards WG et al (2016) Adaptive resistance to therapeutic PD-1 blockade is associated with upregulation of alternative immune checkpoints. Nat Commun 7:10501
11. Yearley JH, Gibson C, Yu N, Moon C, Murphy E, Juco J et al (2017) PD-L2 expression in human tumors: relevance to anti-PD-1 therapy in cancer. Clin Cancer Res 23:3158–3167
12. Appah EO, Ballard BR, Izban MG, Jolin C, Lammers PE, Parrish DD Jr, Marshall DR (2018) A rapidly growing human papillomavirus-positive oral tongue squamous cell carcinoma in a 21-year old female: a case report. Oncol Lett 15:7702–7706
13. Henneman R, Van Monsjou HS, Verhagen CVM, Van Velthuysen MF, Haar NTT, Osse EM et al (2015) Incidence changes of human papillomavirus in oropharyngeal squamous cell carcinoma and effects on survival in the Netherlands Cancer Institute, 1980–2009. Anticancer Res 35:4015–4022
14. Sunshine JC, Nguyen P, Kaunitz G, Cottrell TR, Berry S, Esandrio J et al (2017) PD-L1 expression in melanoma: a quantitative immunohistochemical antibody comparison. Clin Cancer Res. 23:4938–4944
15. Lipson EJ, Lilo MT, Ogurtsova A, Esandrio J, Xu H, Brothers P et al (2017) Basal cell carcinoma: PD-L1/PD-1 checkpoint expression and tumor regression after PD-1 blockade. J Immunother Cancer 5:23
16. Yanik EL, Kaunitz GJ, Cottrell TR, Succaria F, McMiller TL, Ascierto ML et al (2017) Association of HIV status with local immune response to anal squamous cell carcinoma: implications for immunotherapy. JAMA Oncol. 3:974–978
17. Duffield AS, Ascierto ML, Anders RA, Taube JM, Meeker AK, Chen S et al (2017) Th17 immune microenvironment in Epstein-Barr virus-negative Hodgkin lymphoma: implications for immunotherapy. Blood Adv 1:1324–1334
18. Rimm DL, Han G, Taube JM, Yi ES, Bridge JA, Flieder DB et al (2017) A prospective, multi-institutional, pathologist-based assessment of 4 immunohistochemistry assays for PD-L1 expression in non-small cell lung cancer. JAMA Oncol 3(8):1051–1058
19. Hirsch FR, McElhinny A, Stanforth D, Ranger-Moore J, Jansson M, Kulangara K et al (2017) PD-L1 Immunohistochemistry assays for lung cancer: results from phase 1 of the blueprint PD-L1 IHC assay comparison project. J Thorac Oncol 12(2):208–222
20. Gaule P, Smithy JW, Toki M, Rehman J, Patell-Socha F, Cougot D et al (2017) A quantitative comparison of antibodies to programmed cell death 1 ligand 1. JAMA Oncol 3(2):256–259
21. Westra WH (2015) The pathology of HPV-related head and neck cancer: implications for the diagnostic pathologist. Semin Diagn Pathol 32:42–53
22. Taube JM, Anders RA, Young GD, Xu H, Sharma R, McMiller TL et al (2012) Colocalization of inflammatory response with B7–h1 expression in human melanocytic lesions supports an adaptive resistance mechanism of immune escape. Sci Transl Med. 4:127ra137
23. Lyford-Pike S, Peng S, Young GD, Taube JM, Westra WH, Akpeng B et al (2013) Evidence for a role of the PD-1:PD-L1 pathway in immune resistance of HPV-associated head and neck squamous cell carcinoma. Cancer Res 73:1733–1741
24. Ang KK, Harris J, Wheeler R, Weber R, Rosenthal DI, Nguyen-Tân PF et al (2010) Human papillomavirus and survival of patients with oropharyngeal cancer. N Engl J Med 363:24–35
25. Taube JM, Galon J, Sholl LM, Rodig SJ, Cottrell TR, Giraldo NA et al (2018) Implications of the tumor immune microenvironment for staging and therapeutics. Mod Pathol 31:214–234
26. Giraldo NA, Nguyen P, Engle EL, Kaunitz GJ, Cottrell TR, Berry S et al (2018) Multidimensional, quantitative assessment of PD-1/PD-L1 expression in patients with Merkel cell carcinoma and association with response to pembrolizumab. J Immunother Cancer 6:99
27. Pardoll DM (2012) The blockade of immune checkpoints in cancer immunotherapy. Nat Rev Cancer 12:252–264
28. Steuer CE, Griffith CC, Nannapaneni S, Patel MR, Liu Y, Magliocca KR et al (2018) A correlative analysis of PD-L1, PD-1, PD-L2, EGFR, HER2, and HER3 expression in oropharyngeal squamous cell carcinoma. Mol Cancer Ther 17:710–716
29. Munn DH (2011) Indoleamine 2,3-dioxygenase, Tregs and cancer. Curr Med Chem 18:2240–2246
30. Schaer DA, Budhu S, Liu C, Bryson C, Malandro N, Cohen A et al (2013) GITR pathway activation abrogates tumor immune suppression through loss of regulatory T cell lineage stability. Cancer Immunol Res 1:320–331
31. Taube JM, Akturk G, Angelo M, Engle EL, Gnjatic S, Greenbaum S et al (2020) The Society for Immunotherapy in Cancer statement on best practices for multiplex immunohistochemistry (IHC) and immunofluorescence (IF) staining and validation. J Immunother Cancer 8:e000155
32. Luke JJ, Azad NS, Edwards R, Huang SMA, Comprelli A, Monga M et al (2018) Phase 1, open-label, adaptive biomarker trial that informs the evolution of combination immuno-oncology (IO) therapies (ADVISE), a precision IO approach to personalized medicine. J Clin Oncol. 36(15 suppl):TPS3101

Publisher's Note Springer Nature remains neutral with regard to jurisdictional claims in published maps and institutional affiliations.

Affiliations

Farah Succaria[1] · Pia Kvistborg[2] · Julie E. Stein[1] · Elizabeth L. Engle[3,4] · Tracee L. McMiller[4,5] · Lisa M. Rooper[6] · Elizabeth Thompson[4,6] · Alan E. Berger[5] · Michiel van den Brekel[2] · Charlotte L. Zuur[2] · John Haanen[2] · Suzanne L. Topalian[4,5] · Janis M. Taube[1,3,4]

1 Department of Dermatology, Johns Hopkins University School of Medicine, Baltimore, MD, USA

2 Netherlands Cancer Institute, Amsterdam, The Netherlands

3 Department of Oncology, Johns Hopkins University School of Medicine, Baltimore, MD, USA

4 Johns Hopkins Bloomberg–Kimmel Institute for Cancer Immunotherapy and Kimmel Cancer Center, Baltimore, MD, USA

5 Department of Surgery, Johns Hopkins University School of Medicine, Baltimore, MD, USA

6 Department of Pathology, Johns Hopkins University School of Medicine, Baltimore, MD, USA